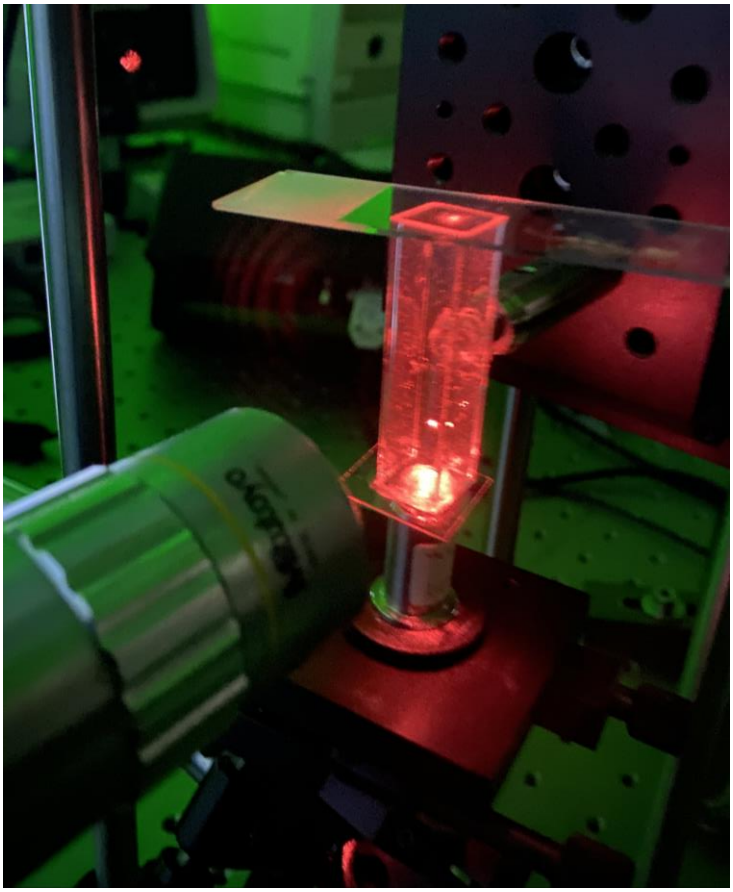

OPTICAL LEVITATION OF TRANSPARENT MICROSPHERES

Facultad de Ciencias
Universidad de La Laguna

María García Alonso

Universidad de La Laguna
Facultad de Ciencias
Grado en Física
Curso 2020-2021

Tutor: Dr. Leopoldo L. Martín

"The more trapped we are by the world, the more difficult it is for us to catch it"

Edgar Morin

Index:

Resumen

El objetivo del presente trabajo fue el estudio del funcionamiento de una trampa óptica. Para ello, con la utilización de un láser de Titanio-Zafiro, bombeado por un láser DPSSL de 532 nm, se logra levitar una microesfera de sílice en una cavidad debido a las fuerzas de presión de radiación. Las fuerzas ejercidas sobre la microesfera son la fuerza de gradiente y la fuerza de scattering. La fuerza de scattering tiene como dirección la dirección de propagación del haz y la fuerza de gradiente apunta transversalmente hacia la región de alta intensidad del haz.

Además de los dos láseres mencionados, otros materiales necesarios para la realización del estudio fueron: un filtro de densidad neutra gracias al cual a pesar de utilizar el láser a alta potencia (donde fluctúa menos) se logra la potencia correcta en la trampa, un fotodiodo conectado a un osciloscopio; un par de espejos para redireccionar el haz láser y el sistema de la trampa óptica.

Para poder realizar la captura de la microesfera es necesario alinear, previamente. los elementos del banco óptico, para que el haz del láser pase de forma perpendicular a la mesa al atravesar la cavidad donde se vierten las microesferas en seco con la ayuda de una pipeta. Se intenta, a la hora de soltarlas, hacerlo de forma que pasen por el spot del láser (donde focaliza) ya que es ahí donde se confinan.

Así mismo, para poder observar la captura de las microesferas es necesario focalizar con anterioridad, en el spot, la cámara utilizada para las grabaciones del movimiento de la muestra. Como último preparativo antes de la realización del experimento, hay que maximizar la salida del láser Ti:Sapp con el movimiento controlado de los espejos internos del mismo; este proceso debe repetirse al comienzo de cada sesión de laboratorio.

Una vez preparado el lugar de trabajo se realizan varios vídeos de la microesfera levitando para cada potencia del láser de bombeo, así como la grabación en el osciloscopio de la intensidad del láser. Esto último se logra conectando un fotodiodo, sobre el que incide una reflexión del haz láser causada por el filtro de densidad neutra situado en el banco óptico, al osciloscopio.

Dado que el objetivo era el estudio de la relación entre las oscilaciones de la posición de la muestra y las fluctuaciones del láser, se realizaron manipulaciones de los datos obtenidos en el laboratorio para poder trabajar con ello. En el caso de los vídeos de la microesfera, primeramente, fueron tratados con el software "Avi Converter", para dividirlos en fotogramas y obtener así una imagen de la microesfera cada cierto intervalo de tiempo; posteriormente, con un programa en Mathematica, se obtuvieron las coordenadas de la posición de la microesfera para cada uno de los fotogramas anteriores. Para el caso de los datos de intensidad obtenidos con el osciloscopio se utiliza la relación entre los voltajes proporcionados por el osciloscopio y la potencia del láser de bombeo, así como la relación de la potencia del láser tras el filtro y de la potencia del láser de bombeo, para terminar obteniendo de los voltajes dados la potencia del láser en la trampa óptica.

Al representar los datos de posición de la microesfera según las distintas potencias del láser de bombeo se observó que presentaban una cierta inclinación debido a que la cámara, en el momento de las grabaciones, presentaba una rotación hacia un lateral. Por ello se seleccionó un eje para establecer el ángulo de inclinación de los datos y poder rotarlos. Solventada dicha desfiguración de los datos se pudo ver en que, a partir de una cierta potencia del láser de bombeo, las posiciones de la microesfera dejaban de estar concentradas en una zona y presentaban una distribución elíptica. Para establecer si este hecho era producto de las fluctuaciones del láser se procedió a realizar un análisis del espectro de potencias de los datos.

El espectro de potencias de una señal proporciona el número de veces que dicha señal oscila por segundo. Al aplicar el espectro sobre los datos de posición en eje X e Y por separado y sobre los de la potencia del láser en la trampa, se observó que solo los datos del eje Y obtenidos a baja potencia del láser de bombeo presentaban un patrón de oscilación similar al del láser en la trampa, por lo que las fluctuaciones del láser no son las responsables de la anómala situación. Esto lleva a pensar que esta dispersión de la posición de la microesfera en suspensión se deba a un cambio en las propiedades del láser en la cavidad, producido por el efecto de lente térmica en el filtro de densidad neutra. Dicho efecto provoca un cambio en el índice de refracción del material, debido a que este presenta un gradiente de temperatura al haber absorbido parcialmente el haz láser. No se pudo concluir si este efecto era el único causante o si el filtro presentaba dicho efecto al faltar datos para realizar el cálculo.

De las representaciones gráficas del espectro también se puede concluir que, cuanto mayor es la potencia del láser de bombeo, menos oscilaciones de la posición por segundo presenta la microesfera pero que la amplitud de esa oscilación para el eje Y aumenta.

Los datos obtenidos en el presente trabajo permiten abrir nuevos frentes de estudio, para comprender qué características del haz láser producen esta alteración de los datos, así como ver cómo afectan estas a las fuerzas de scattering y gradiente, generadoras de la captura de la microesfera.

Keywords:

Microspheres, pump laser, neutral density filter, thermal lensing, power spectrum.

Introduction

Resumen:

La pasión o incertidumbres que ha tenido la humanidad sobre qué es la luz la ha conducido al entendimiento de la misma como una onda-corpúsculo y así, continuando con el legado de los anteriores científicos se creó el láser para seguir investigando la luz. Con él se pueden mover y levitar partículas micrométricas dieléctricas gracias a las fuerzas ópticas. Así mismo, esta manipulación tiene una aplicación práctica para biólogos o médicos para aplicar fuerzas controladas en células vivas.

Since the ancient times the human being has been wondering about what it is and where the light comes from. How is it that we can see our surroundings? Initially the answers to these questions were philosophical and religious, focusing on vision. We have the Greek myth of Prometheus for example, who stole fire from the gods to give it to humans.

Later, in 1619, Johannes Kepler looking at the direction of comet tails, which is always opposite to the position of the sun, proposed that light could exert mechanical forces on the particles. Therefore, mankind asked more questions about the light. [1]

Then, in 1873, with James Clerk Maxwell and the advent of electrodynamics it was theoretically proved that the light could exert optical forces, named radiation pressure. It was also shown that in some cases the electromagnetic field could propagate as a wave, realizing that light is such a wave [2].

Later, with Einstein and Planck, within the framework of quantum mechanics, it was explained that light also consisted of quanta behaving as a flow of corpuscles called photons (which, like matter particles, can exert pressure on objects, and even transfer momentum) [1].

With all this and the laser creation, arrives Arthur Ashkin in 1970 [3]. Who demonstrated that optical forces could move and levitate micrometric dielectric particles. The use of laser capture and manipulation techniques gives a remarkable

degree of control over the dynamics of small particles, making it highly useful in atomic physics and biology.

For example, in biology it can be used to remotely apply controlled forces on living cells. Among other things, they have helped researchers unravel the complex elasticity and folding dynamics of DNA, RNA, proteins and other long-chain "biopolymers". In these experiments, the biopolymers are typically manipulated from both ends either by suspending them between an optical trap and a surface, or between multiple traps. Data obtained using optical tweezers complement measurements made using other techniques for measuring the forces on single molecules – including atomic-force microscopy (AFM) [4].

Objectives

Resumen:

El objetivo del presente trabajo es el estudio del funcionamiento de una trampa óptica. Para ello se realiza un experimento cuyos elementos principales son un láser de Titanio Zafiro y las microesferas de sílice.

El estudio consiste en una recogida de datos de la posición de la microesfera en levitación y de la intensidad del láser en la trampa para, una vez obtenidos todos los datos, poder relacionar la oscilación en posición del cuerpo de estudio con la fluctuación del láser.

The objective of the present work is the study of the operation of an optical trap. For this, an experiment is carried out whose main elements are a Titanium doped Sapphire laser and silica microspheres.

The study consists of collecting data on the position of the microsphere in levitation and the intensity of the laser in the trap so that, once all the data have been obtained, the oscillation in position of the study body can be related to the fluctuation of the laser.

Theoretical background

Resumen:

La respuesta de los objetos sobre los que actúa la fuerza óptica depende tanto de la potencia total incidente como del índice de refracción, de la geometría y del tamaño relativo del objeto respecto a las dimensiones características del haz.

Si se hubieran elegido partículas no-esféricas se dificultaría el trabajo al tener que considerar una rotación de la misma debida al torque inducido.

Según el diámetro del cuerpo de estudio sea mayor o menor que la longitud de onda del haz incidente se tienen tres regímenes diferentes con una aproximación a seguir, por lo que conocer las dimensiones de los distintos elementos es importante, así como las propiedades generales del material.

Se trabajará en el régimen de Mie ya que el radio de la muestra empleada en el trabajo es mayor que la longitud de onda del láser utilizado.

The optical trap technique consists of the use of highly focused light beam capable of trapping small neutral particles around the focal zone, based on radiation pressure forces [5].

More specifically, there is an optical force acting on the surface of the object due to the change of momentum of the light product of the reflection and refraction of the laser beam [6].

The response of the study objects to a given light distribution depends on the total incident power, the refractive index, the geometry and the relative size of the object with respect to the wavelength of the beam [1].

If in the study, instead of having spherical particles, they were non-spherical particles, the rotation induced by a torque should also be considered, since these particles in addition to the optical force would experience an induced torque, which is generated as a result of an imbalance in the optical force profile [6].

So, it would be difficult to study the movement of the bodies by varying the optical force with the angle of incidence during rotation.

Once the choice of the type of geometry of the study particles has been explained, the three regimes are introduced according to the relative size of the radius of the spheres and the wavelength of the beam used.

In the first instance the Mie regime is presented, which is the one corresponding to when the size of the particle is greater than the wavelength of the incident light.

In this regime, the conservation of the momentum model or optical ray optics is applied, where the total light is decomposed into individual rays (each with the appropriate intensity, direction and state of propagation). Each of these rays has the characteristics of a plane wave of zero wavelength that can change polarization at dielectric interfaces according to Fresnel formulas [1, 7, 8].

In this work the ray optics method will be followed, another added complication if non-spherical particles had been used is that they cannot be described by geometric relationships, while spherical particles are of regular shape so that they can used it to obtain the transfer of the momentum [6].

Then the Rayleigh regime, where the size of the particle is substantially less tan the wavelength of the laser. In this case the trapped particles can be considered as an induced dipole [7].

And between these regimens, where the size of the particle is comparable to the wavelength we have the regimen studied by Ashkin, in which neither the optics of the rays nor the approximation to a dipole are valid, and more complex electromagnetic theories would be needed [7].

Finally, the capture forces experienced by the study bodies are described, which depend on the intensity, power and wavelength of the laser beam, and the size and shape of the particles [7].

The net force that the particle experiences can be divided into two, the scattering force and the gradient force.

To visualize these force components, imagine a sphere with a high refractive index placed outside the axis of a slightly focused Gaussian ray, as shown in Figure 1.

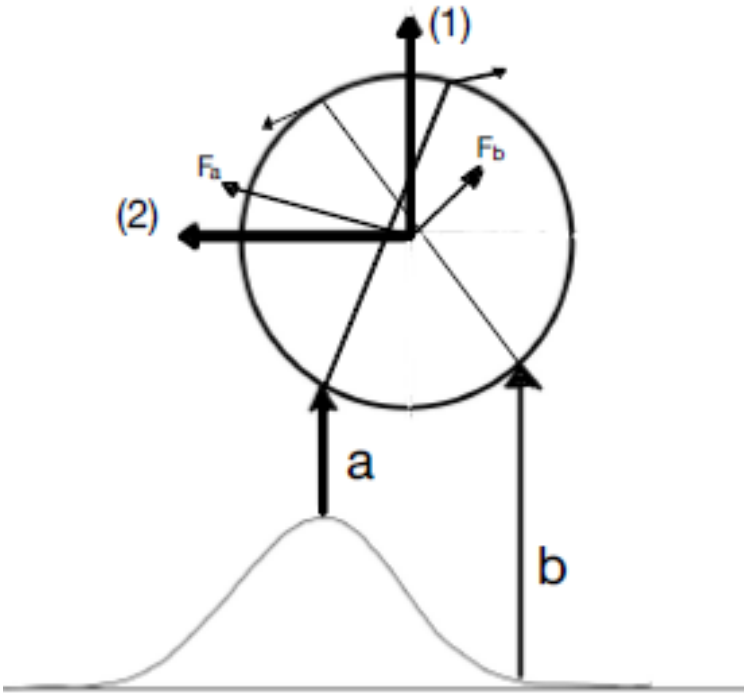

Figure 1: schematization of the forces in the microsphere due to a pair of rays, a and b.

A pair of rays are considered, a and b, striking the sphere symmetrically about its vertical axis. The first ray, a, is of greater intensity than ray b due to the irradiance profile of the Gaussian beam, which is symmetric around the center of the ray and decreases as the distance from the center of the beam perpendicular to the direction of propagation increases.

Ignoring the reflections, most of the rays are refracted through the surface of the sphere, which gives rise to the forces F_a and F_b in the direction of the momentum change, of which the first is greater than the second due to the intensities of the rays [5].

And it is by adding all the symmetric pairs of incident rays in the sphere that it is observed that the net force is decomposed into the forces (1) of scattering and (2) of gradient, as already mentioned [5].

The scattering force is produced by the striking of the laser photons on the body along its direction of propagation. While the gradient force is produced by the intensity

gradient of the light and points transversely towards the region of high intensity of the beam [5].

Then, depending on the regime, these forces will have different expressions when making the pertinent approximations.

Specifically, in Rayleigh regime, the scattering force is due to absorption and reradiation of light by the dipole. [9] For a sphere of radius r, this force follows the equation:

$$F_{scatt} = \frac{I_0 \sigma n_1}{c}$$

Being $\sigma = \frac{128\,\pi^5 r^6}{3\lambda^4} \cdot \left(\frac{m^2-1}{m^2+2}\right)^2$, $m = \frac{n_2}{n_1}$

Where I_0 is the intensity of the incident light, σ is the scattering cross section of the sphere, n_1 is the index of refraction of the medium, is the speed of light in vacuum, m is the ratio of the index of refraction of the particle to the index of the medium and λ is the wavelength of the laser [9].

And the time-averaged gradient force arises from the interaction of the induced dipole with the inhomogeneous field [9]:

$$F_{grad} = \frac{2\pi a}{c\, n_1^2} \nabla I_0$$

Where $a = n_1^2 r^3 \left(\frac{m^2-1}{m^2+2}\right)$ is the polarizability of the sphere.

On the other hand, since individual rays are considered in the Mie regime, the forces of Dispersion and Gradient on the sphere are the sum of the forces produced by each ray. The expressions for such contributions are [8]:

$$F_{scat} = \frac{n_1 P}{c}\left\{1 + Rcos(2\theta) - \frac{T^2[\cos(2\theta-2r)+Rcos(2\theta)]}{1+R^2+2Rcos(2r)}\right\}$$

$$F_{grad} = \frac{n_1 P}{c}\left\{Rsin(2\theta) - \frac{T^2[\sin(2\theta-2r)+Rsin(2\theta)]}{1+R^2+2Rcos(2r)}\right\}$$

Where P is the power of the incident ray at an angle θ, r is the angle of refraction and R and T are the Fresnel reflection and transmission coefficients form the surface at angle θ [8].

At this point the refractive index should be mentioned since if a particle with a low index is located outside the axis it will be expelled from the beam when the refraction is reversed through the particle, Fa<Fb [5].

When the index of refraction of the particle is greater than the index of refraction of the medium, the optical force arising from refraction is in the direction of the intensity gradient. While otherwise the force is in the opposite direction of the intensity gradient [9].

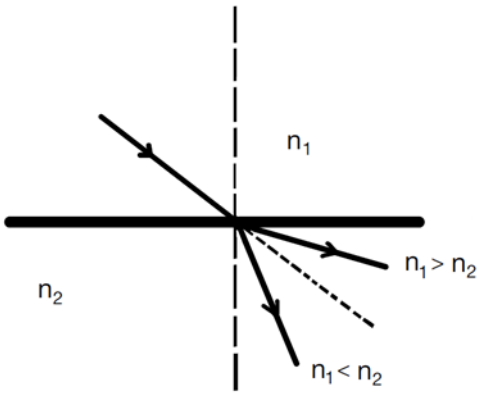

Figure 2: refraction of a beam as it passes through the medium according to the refractive index.

Setup

Resumen:

Los elementos utilizados para el experimento se situarán sobre un banco óptico, correctamente fijados para no tener problemas con desalineamientos.

El sistema consta de un láser de zafiro dopado con titanio que es bombeado por un láser de bombeo, de un par de espejos para redirigir el haz láser, de filtros de densidad neutra para bajar la potencia del haz en la trampa, de un fotodiodo conectado a un osciloscopio para medir las fluctuaciones del láser y un subsistema de trampa óptica.

El subsistema consta de una cavidad, una lente parabólica para focalizar el láser y una cámara para la grabación del movimiento de los cuerpos de estudio.

Before starting the experiment, let's talk about the elements that are used for it. Next, in figure 3, the used objects placed on the optical bench can be seen; likewise, for a better visualization of the optical path travelled by the laser, figure 4 can be seen, which schematically represents the elements from a top view.

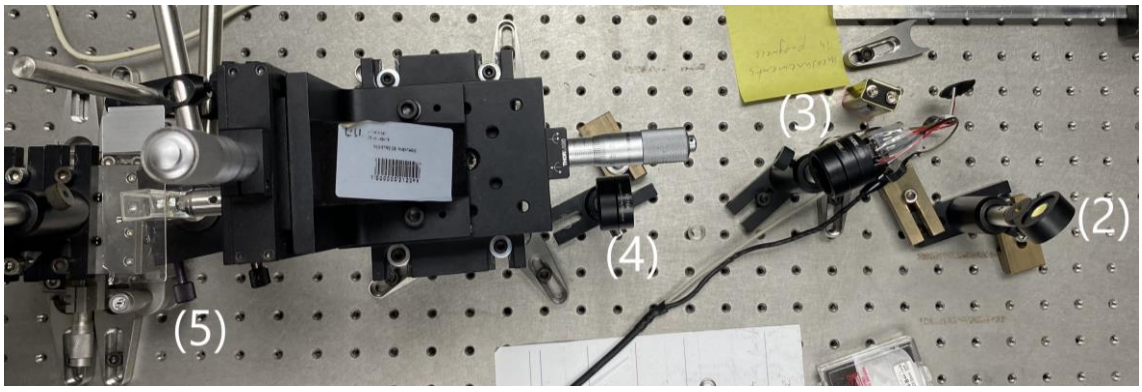

Figure 3: optical bench.

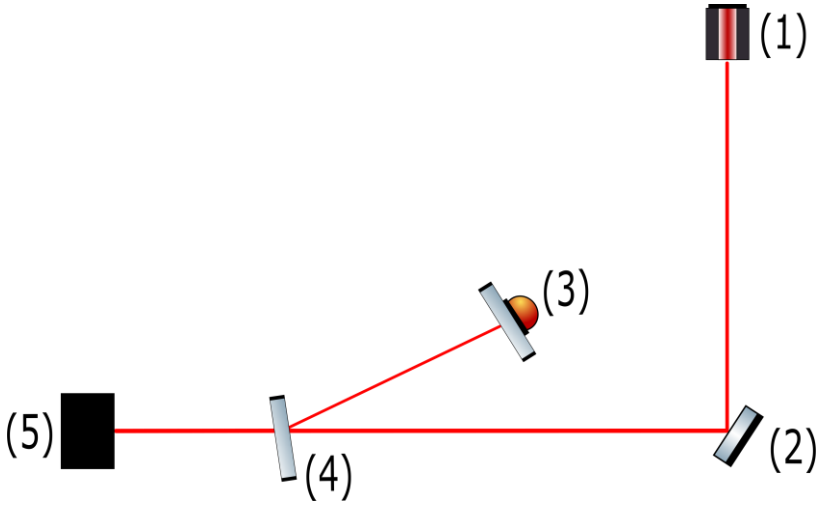

Figure 4: optical bench diagram.

The laser path will be described using figure 4 as a guide. It starts at number (1), which corresponds to the laser source, which emits in the direction of a mirror. Said mirror redirects the beam towards a neutral density filter (ND) (4) that will reflect a small amount of light onto a photodiode (3) to be measured with the oscilloscope connected to it, while the rays that pass through the filter are directed to system (5). The last system is marked as a set since a plane change will be made to see its components. This system consists of a mirror that redirects the beam to the vertical axis, where there is a lens that will focus the laser to be used in the optical trap (see figure 5).

Once the path of the beam is understood, the elements used are detailed below.

A capture laser is required which provide single mode output with good aiming and low power fluctuations [9]. A Titanium doped Sapphire (Ti:Sapp) laser is used, which is a tunable laser in the near infrared region. This Ti:Sapp is optically pumped by a 532 nm Solid State Diode Pumped Laser (SSDPL). The Ti:Sapp output is maximized by tweaking the cavity mirrors in order to achieve a more stable output. The most efficient trapping settings are: Ti:Sapp power of 288 mW and pumping at 4,25 W with the SSDPL so that later with the use of filters, lower it to the required power.

Then the mirrors used to redirect the laser beam are dielectric multilayer half-inch mirrors, used due to their high reflectance design with high threshold of laser damage.

The use of a ND filter (4) within the system is due to the fact that the laser at low power fluctuates much more than at high power, which could cause a suspended

microsphere to fall during measurements. For this reason, it was preferred to use the laser at high power and then by means of a filter of optical density 2 to achieve a final power of 50 mW in the optical trap with the settings in the lasers mentioned above.

Adding the filter also allowed a reflection of the laser to be used to simultaneously measure the variations in laser power with the oscilloscope and record the sphere levitating.

In figure 5 the system (5) is seen, which consists of a mirror like those mentioned above, which directs the laser beam to the 15,55 mm focal length parabolic lens (5b) that focuses the laser in the cavity. This cavity is a cuvette: an empty rectangular prism without a cap and with a perforation in the base covered with a microscope coverslip so that the beam passes through a thinner all and has less loss or deviation.

It is in the cavity where the microsphere capture process will take place, so the camera (5c) will be focused on the focus of the ascending laser beam and thanks to the Sharpcap program the event can be observed and recorded.

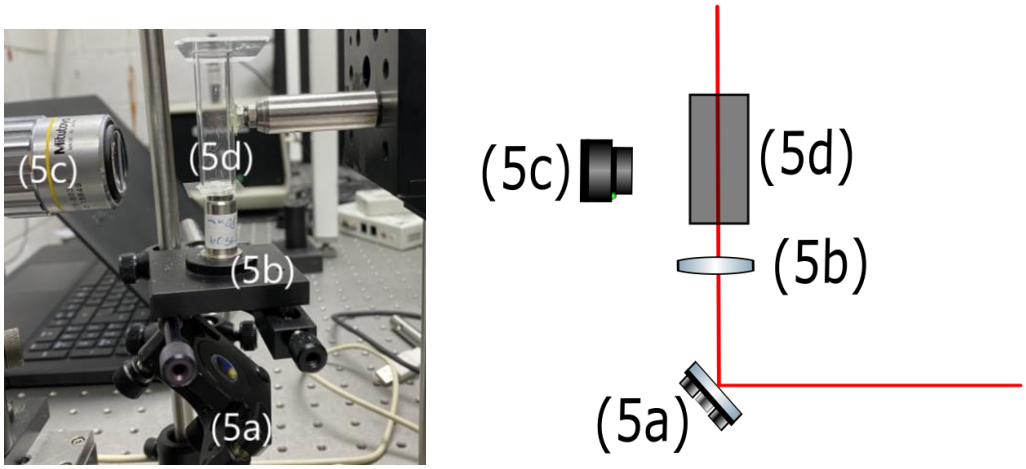

Figure 5: decomposition of the system (5) of figure 4.

Methodology and experimental procedures

Resumen:

Para llevar a cabo el experimento primero se han de alinear los elementos del banco óptico para lograr que el haz láser pase de forma perpendicular a la mesa cuando atraviese la cavidad. Así mismo, como preparativo previo está el enfoque de la cámara al foco del láser para que solo sean necesarios pequeños cambios en su altura, al ser el foco el lugar donde la microesfera se mantendrá confinada.

Posteriormente y antes de cada sesión de laboratorio se ha de maximizar la salida del láser Ti:Sapp. Una vez hechos todos los preparativos las microesferas serán vertidas en seco en la cavidad con la ayuda de una pipeta, y cuando se logre atrapar una en la trampa óptica se procederá a grabar su movimiento simultáneamente con las oscilaciones del láser en el osciloscopio.

The experiment is carried out in the Laser Spectroscopy and High Pressure Laboratory. The first step in carrying out the study consists of aligning the mirrors in such a way that the beam passes perpendicular to the ground when it passes through the cavity.

At the beginning of each laboratory session it is necessary, first, to turn on the laser following the protocol available on the laboratory bench. Once the shutter is open, proceed as mentioned in the previous section, to maximize the output of the Ti:Sapp laser by adjusting the cavity mirrors.

In the first laboratory session, once the laser is stable and correctly aligned, it is necessary to focus the camera at the distance the laser focal point, in order to have it in position when the experiment is carried out. To do this, the cavity is positioned in such a way that the closest wall to the camera interrupts the path of the beam. Its known that the laser passes through the wall correctly (tangent to the normal of the surface) when it is illuminated with greater intensity. Subsequently, looking for the refractions that occur in the lower edge of the cavity, once the camera is focused there; when the experiment

is carried out, it will only be necessary to change the camera in height and minimum focus adjustments will be made.

When all the preparations are made, the experiment will begin. As has been previously announced, silica microspheres will be used for the experiment. With the help of a pipette, the microspheres will be released into the cavity, covering it immediately. The idea is to let them fall where the laser rises so that some of theme pass through the spot of the laser and levitate due to the compensation of the forces exerted on it.

In the beginning another method was used to pour the microspheres, which required a suspension in isopropanol, resulting in many failed attempts. We think it could be due to humidity and that the microspheres forming too heavy conglomerates for the capture system. For this reason, it was decided to use dry microspheres.

Even son, an image of the sample of the microspheres in isopropanol after it has evaporated is shown in figure 6. This was taken with stereoscopic microscope.

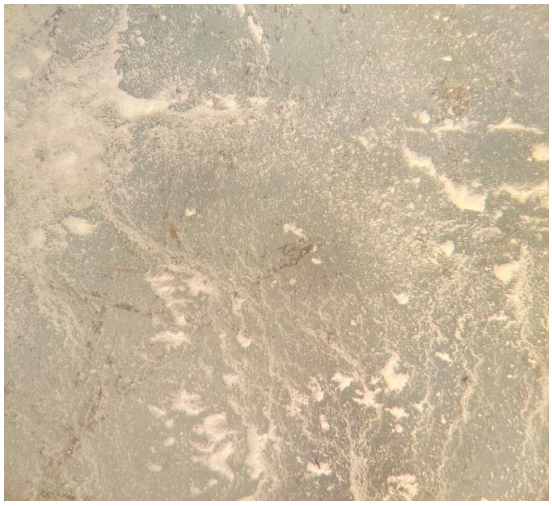

Figure 6: microspheres dissolved in isopropanol after having been evaporated.

Once a microsphere is trapped in the optical trap, its movement is recorded. For this, a Philips camera is used connected to the laboratory computer in which the SharpCap program is used, while the variations in laser power in the photodiode are recorded on the oscilloscope. About 3 minutes of recording are done for each data set. Once the video is saved, the pumping power of the beam is changed and the movements of the microsphere and the variations in laser power are recorded again. As the pump's

laser power increases or decreases, make sure that the microsphere continues to appear on the computer; otherwise, the height of the camera will need to be adjusted.

All variables will be noted, that is, for each video the height of the camera at which it was made and the pumping power will be indicated.

Results and discussion

Resumen:

A la hora de representar los datos de posición de la microesfera se vio que estos presentaban una inclinación, por ello se estableció un eje y se rotaron para poder observar la oscilación en los ejes horizontal y vertical. También, se trataron los datos proporcionados por el osciloscopio para obtener la oscilación de la potencia del láser en la trampa.

Se encontró que, a partir de una cierta potencia, 4.25 W, del láser de bombeo la posición de la microesfera dejó de estar concentrada en una zona y que describía movimientos elípticos. Este hecho no parece deberse a las fluctuaciones del láser, sino que es probable que se deba a un cambio de las características del haz en la trampa provocado por el efecto de lente térmica, el cual se produce por una absorción parcial del láser por el filtro de densidad neutra. Esto provoca en el filtro un gradiente de temperatura que altera su índice de refracción, así como la forma de sus paredes.

También se observó que la oscilación principal del eje X y el eje Y coincidían, así como que la microesfera oscilaba más lentamente según se aumentaba la potencia del láser de bombeo, haciéndose mayor la amplitud de esta oscilación para el eje Y.

This section will describe the data analysis and the relevant information.

To obtain these data, a processing of the videos taken is required. Once the videos were downloaded to the computer, with the use of the “Avi Converter” software, they were decomposed into still frames to have images of the position of the sphere for every certain time. These frames were then processed in Wolfram Mathematica 11 with a command called “IntensityCentroid” that gave coordinates to the centroid of a given image. The positions of each centroid were given in pixels and stored in data files. In addition, Mathematica was also used to find the conversion factor from pixels to microns, for this the camera was focused on the front wall of the cavity, the height given by the micrometric screw was noted and a photo was taken, then the screw was

moved about 250 microns and took another photo. By changing the position, in pixels, of a mark on the wall, the ratio of pixels to microns can be obtained.

The subsequent work with the data was carried out with Python, the pixel positions are converted to microns with the scale obtained in Mathematica. The height of the chamber in the laboratory was not added to the data shown, so the values on the axes correspond to the positions in the reference system of the camera in microns. All values were taken with the camera at the same height.

In figure 7, the values of the position of the microsphere obtained for different power of the pump laser are shown. Each potted point corresponds to the centroid of the microsphere in one frame of the video.

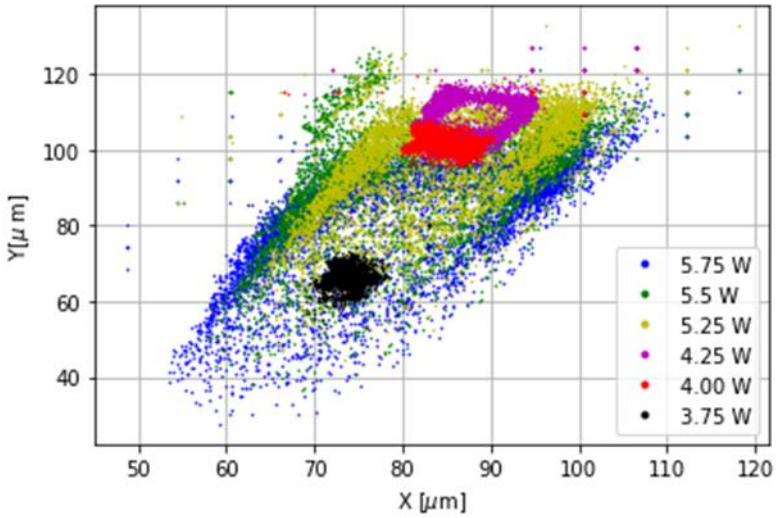

Figure 7: representation of the microsphere positions according to the power of the pump laser.

Once the corresponding representation was made, the tilt of the camera is noticed, so to be able to work with the data, these must first be rotated. To do that, the highest and lowest points are selected and a line is drawn indicating the steepness of the data and how much it should be rotated. The selected points are shown in figure 8. And the data once rotated can be seen in figure 9.

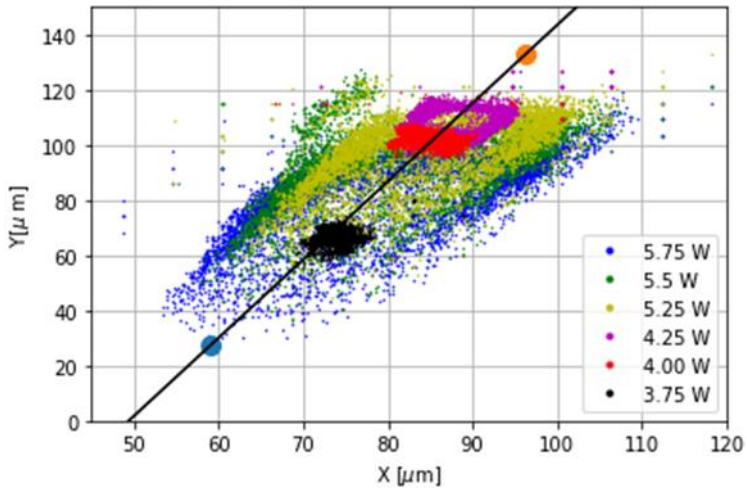

Figure 8: representation of position data indicating the maximum and minimum on the axis Y.

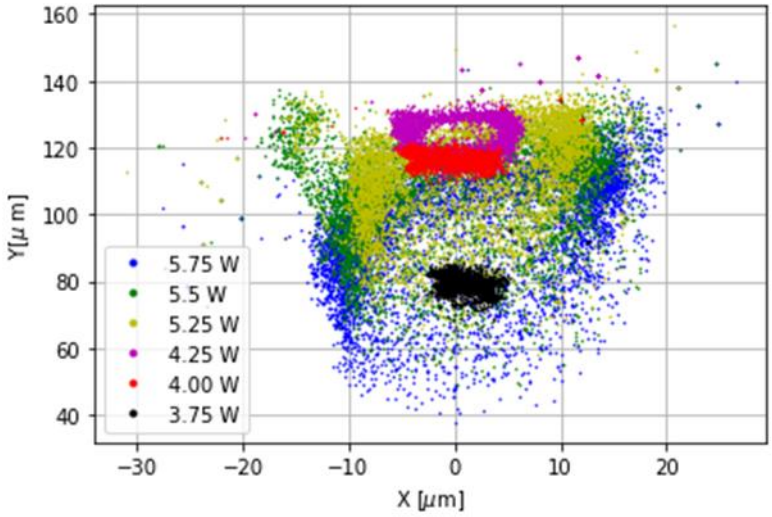

Figure 9: representation of the positions of the microspheres once rotated according to the power of the pump laser.

If you look at the three groups with the lowest power (black, red and magenta) you can see that as the power increases so does the height at which the microsphere is located. But if you look at the three with the highest power this does not happens.

Likewise, it is seen that the lower the power, the more concentrated the points are or, the lower the power, the less amplitude of movement the microsphere has. The event can be seen better in figure 10, where each power has been represented separately.

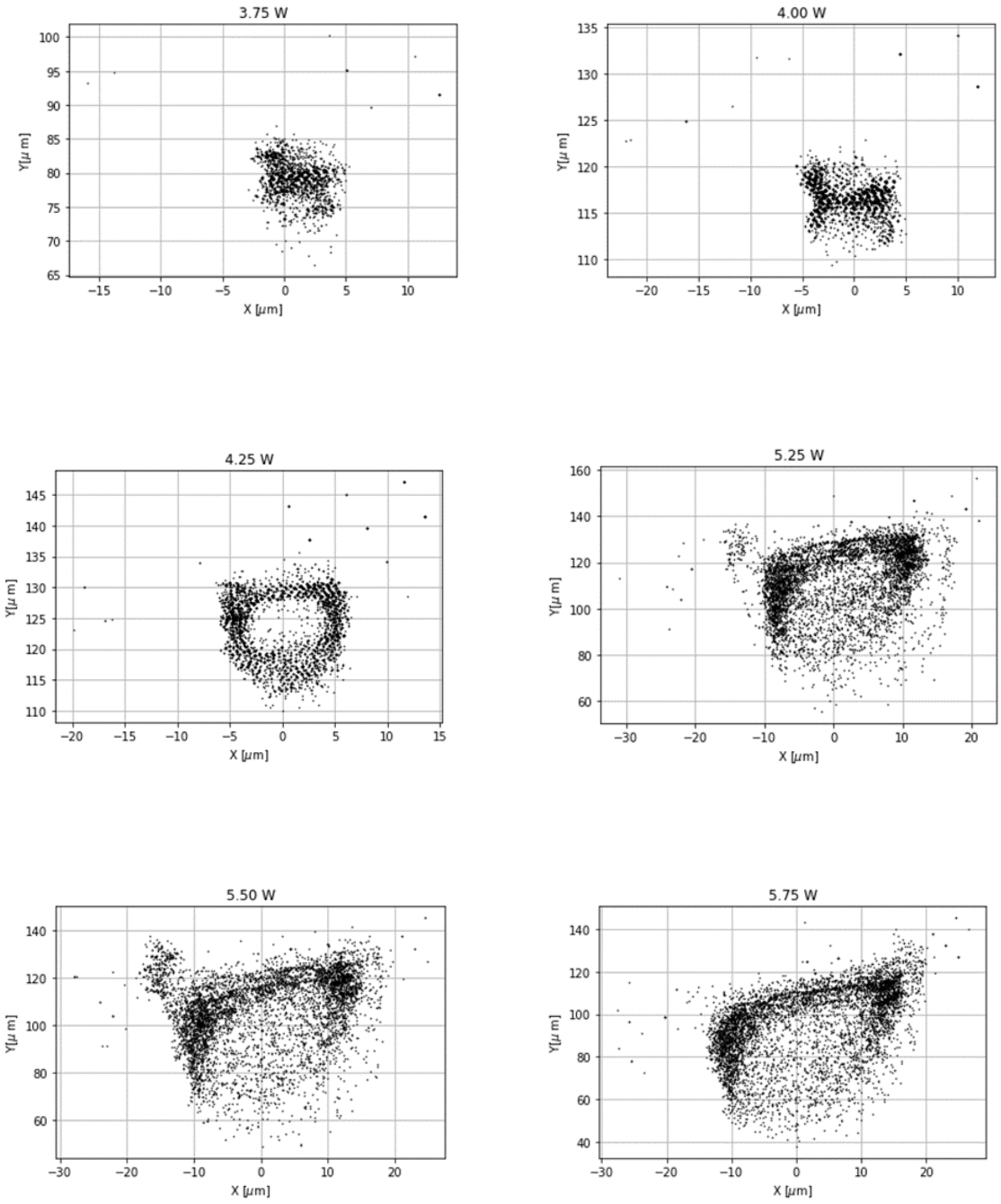

Figure 10: separate representation of the microsphere positions according to the laser pump power.

A possible cause of this very different distribution of microsphere positions is the hypothesis that the thermal lens effect occurred in the Neutral Density filter used in the experiment. The thermal lensing effect occurs when part of the energy in a light beam is absorbed by a semi-transparent material. Due to the absorption of the beam, a thermal distribution occurs that induces a local change in the refractive index of the medium by a factor dn/dT. As the intensity profile in the present experiment is

Gaussian, the temperature increase of the material occurs radially from the beam's axis of propagation. This means that, in the material, the region closest to the axis of propagation has a temperature slightly higher than that of the edges, producing a thermal gradient that originates the thermal lens [10]. Furthermore, this gradient induces an inhomogeneous tension in the filter, causing the center to be compressed and the ends faces bulge out, causing the filter to act as a positive lens [11], shown exaggeratedly in figure 11. Any wavefront propagating through the material will suffer a distortion in its intensity profile due to the transverse phase shift [10].

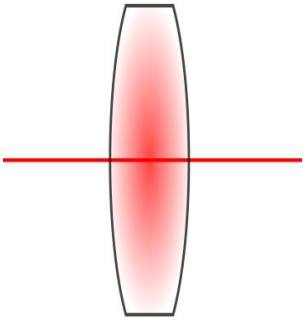

Figure 11: thermal lens effect illustration.

To see if the filter has the effect of a thermal lens and, therefore, could be the cause of the results obtained, another experiment should be carried out, in which, with the use of one or two lasers (one that causes the thermal lens and another, the probe laser), the divergence of the beam or the intensity drop in the center of the beam would be measured. This is something that couldn't be done simultaneously in the present study since if the intensity of the laser in the trap were measured while the sphere levitated, it would fall, and at the time this hypothesis was raised, the lasers in the laboratory were changed. In the absence of this verification, it has been assumed that the filter has this effect and below is shown, for an aberrant theoretical model, the equation that describes the intensity of the laser after the filter at time t [12]:

$$I(t) = I(0)\left\{\left[1 - \frac{\theta}{2}tan^{-1}\left(\frac{2mV}{[(1+2m)^2+V^2]\left(\frac{t_c}{2t}\right)+1+2m+V^2}\right)\right]^2 + \left[\frac{\theta}{4}\,ln\left(\frac{\left[1+\frac{2m}{\left(1+\frac{2t}{t_c}\right)}\right]^2+V^2}{(1+2m)^2+V^2}\right)\right]^2\right\}$$

Where:

$m = \left(\frac{\omega_{1p}}{\omega_e}\right)^2$ indicates the degree of mode mismatch of the test beam and the excitation beam, but since the excitation and sample lasers are the same for this experiment then $m = 1$; where ω_{p1} and ω_e are the radius of the focus of the test and excitation laser beam in the sample respectively, which in this case are equal.

$V = \frac{Z_1}{Z_c}$ having that Z_1 is the distance from the waist of the test beam to the sample and Z_c is the confocal distance of the test beam.

$\theta = -\frac{P_e\, A_e\, l_0}{k\, \lambda_p}\left(\frac{dn}{dT}\right)_p$ is the thermal phase change of the test beam after passing through the sample; where P_e is the excitation beam power, A_e is the optical absorption coefficient, l_0 is the thickness of the sample, k is the thermal conductivity, λ_p is the wavelength of the excitation beam and $\left(\frac{dn}{dT}\right)_p$ is the thermal gradient of the refractive index in the sample.

$I(0) = \left|\frac{C}{1+j\,V}\right|^2$ is the value of $I(t)$ when t is zero or θ is zero.

The data obtained by the oscilloscope must also be processed to be able to use it, since the information that is needed is that of the laser power in the trap.

To do this, the first step was to measure the fluctuations of the laser with the oscilloscope for each pumping power and that gave us the values in Volts. Then, for each data set, an average was taken and Volts vs Power was plotted in order to make a

fitting and have a relationship between the power of the pump laser and the data of the oscilloscope.

The second step was to measure the laser output power in relation to the pump laser power and also make an adjustment to relate the two. As the laser power in the optical trap is needed, a rule of three was made to obtain it, having previously measured for a laser output power (283 mW) how much it passed through the filter (50 mW).

One the data from the oscilloscope has been related to the power of the pumping laser and latter with the power of the laser in the trap, the first can be related to obtain what is needed.

With the variations of the laser power in the optical trap and the positions of the microsphere, work begins. The data of the positions on the X and Y axis are separated, and the squared module of the Fourier Transform is applied to them to calculate their power spectrum (PS), which will help to know how many times the microsphere oscillates per second and if there is more than one oscillation simultaneously. Therefore, in the representation of the power spectrum, the X axis corresponds to the frequency measured in Hz. Then the Y axis of each representation has been normalized for a better visualization of the variations of the different parameters.

Now the representations obtained for the power spectrums will be analysed. But before starting to particularize with what is observed in each graph, it must be remembered that the deltas mean that the signal oscillates at that frequency, for example look at the largest peak in figure 13, which is somewhat above 6 Hz, this means that the signal (in this case the position of the microsphere) oscillates slightly more than six times per second.

Pump laser power: 3.75 W

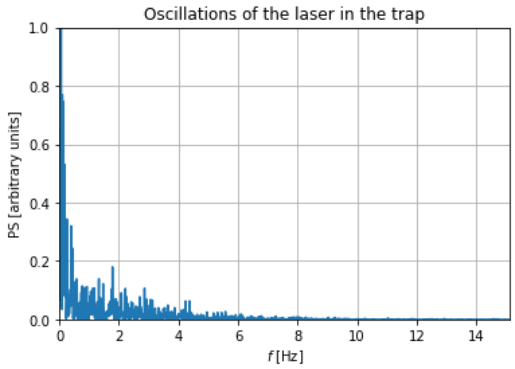

Figure 12: power spectrum representation of the laser power in the trap for a pump laser power of 3.75 W.

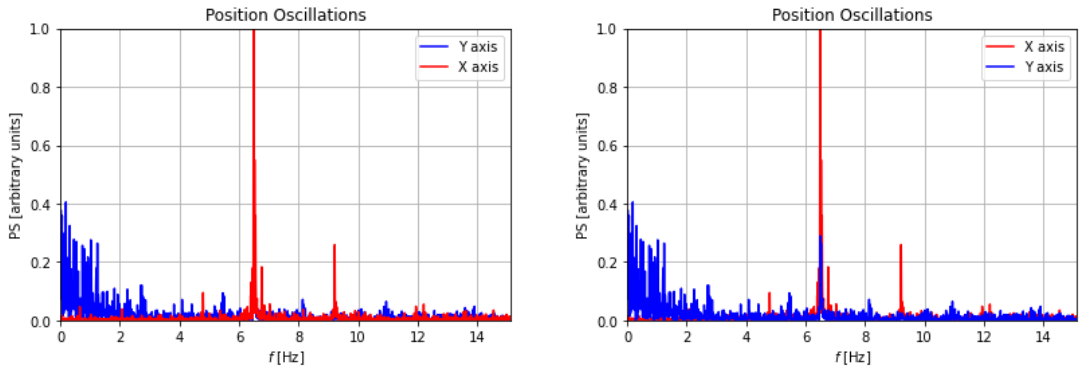

Figure 13: representation of the power spectrum of the positions on the X and Y axes of the microsphere for a pump laser power of 3.75 W.

Pump laser power: 4.00 W

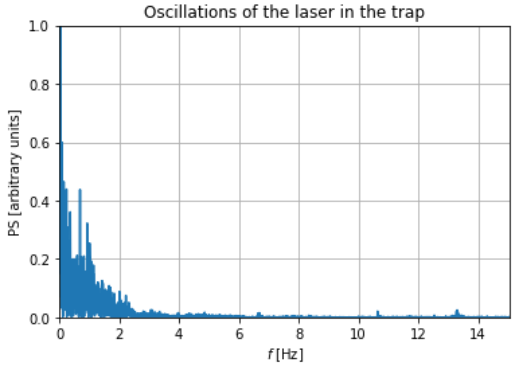

Figure 14: power spectrum representation of the laser power in the trap for a pump laser power of 4.00 W.

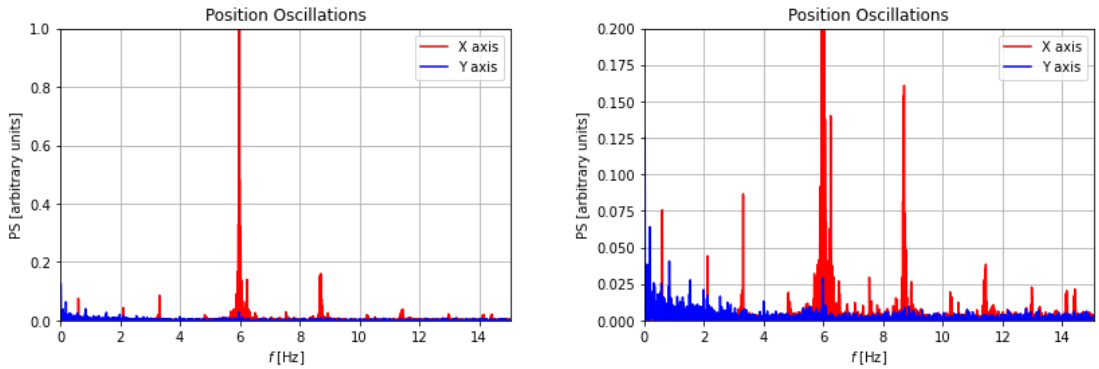

Figure 15: representation of the power spectrum of the positions on the X and Y axes of the microsphere for a pump laser power of 4.00 W.

Pump laser power: 4.25 W

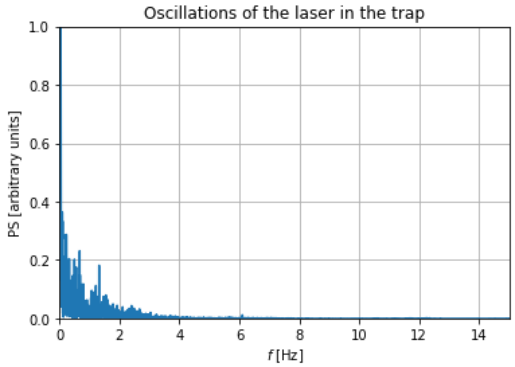

Figure 16: power spectrum representation of the laser power in the trap for a pump laser power of 4.25 W.

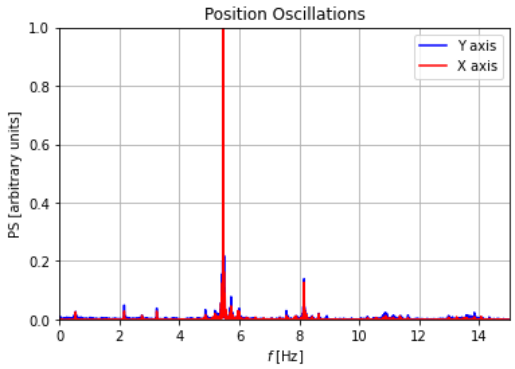

Figure 17: representation of the power spectrum of the positions on the X and Y axes of the microsphere for a pump laser power of 4.25 W.

Pump laser power: 5.25 W

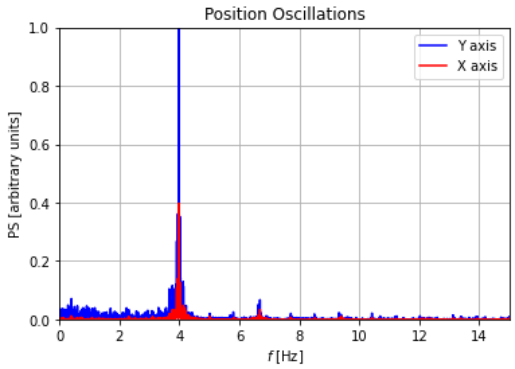

Figure 18: representation of the power spectrum of the positions on the X and Y axes of the microsphere for a pump laser power of 5.25 W.

Pump laser power: 5.50 W

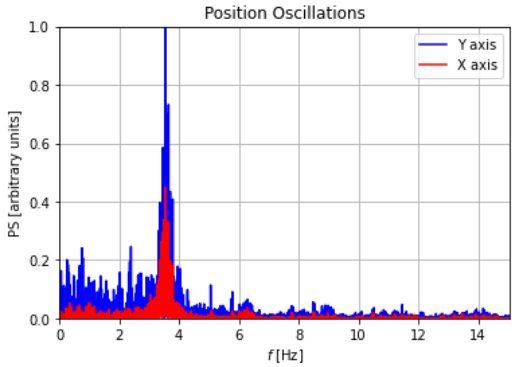

Figure 19: representation of the power spectrum of the positions on the X and Y axes of the microsphere for a pump laser power of 5.50 W.

Pump laser power: 5.75 W

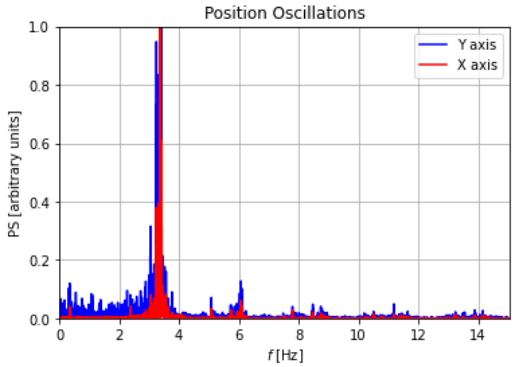

Figure 20: representation of the power spectrum of the positions on the X and Y axes of the microsphere for a pump laser power of 5.75 W.

As can be seen in figures 12 to 15, for the two cases of lower power of the pump laser there is a similar pattern of oscillation for the power of the laser in the trap and for the position on the Y axis. But, as the power of the pump laser increases the contribution of the fluctuation of the laser in the oscillation of the position of the microsphere is no longer visible, as can be seen in figure 16 and 17, and this could be due to the effect of the thermal lens. As in figure 9, where it is observed that from the power of 4.25 W for the pump laser, the positions of the microsphere begin to disperse. Since there is an effect that adds an additional change to the laser intensity in the trap that is unknown. The treatment of the data provided by the oscilloscope is no longer reliable for pump laser powers greater than or equal to 4.25 W.

Likewise, it can be seen in the graphs that the largest peaks corresponding to the movement in the X and Y axis coincide, that is, the main frequency at which the microsphere oscillates in both axes is the same, although with a greater or lesser amplitude. Then, when seeing the evolution of these peaks, it is detected that the amplitude of the characteristic oscillation in the Y axis becomes larger as the power of the pump laser increases. This could be due to the fact that the scattering force is greater the higher the power.

Then if instead of analysing the representations according to the axis of the power spectrum, it is done with respect to the frequency axis, it is observed that the number of oscillations per second of the position, both in X and Y axes, decreases.

Finally, it should be mentioned that the signal, or the position in the X and Y axes, is not periodic, since it only has one important peak without any harmonic. If in the power spectrum the peaks appeared at for example 4, 8, 12, 16…Hz this would indicate that the signal is periodic, but since it does not happen, it implies that it has a certain component of randomness. In addition, the periods, in the real world are never perfect, that randomness is related to the dissipation of the energy and other parameters. But it doesn’t seem like a purely random or chaotic system. Although the chaos would have to be explored.

Conclusions

Resumen:

Esta investigación tenía por finalidad el estudio de la oscilación de la posición de la microesfera según las fluctuaciones del láser. El objetivo se cumplió parcialmente, ya que a la hora de analizar los datos se observó que varios conjuntos de datos (según la potencia del láser de bombeo) presentaban unas características anómalas, esto es que la microesfera al levitar oscilaba en círculos. Lo que llevó a la búsqueda de una posible explicación para esta anomalía y ver si había un patrón en ella. Se puede concluir que el efecto de lente térmica es probable, aunque no se tiene una teoría justificada que explique las oscilaciones en la posición de la microesfera ya que no se deben directamente a las fluctuaciones del láser. Sería necesario realizar un estudio en profundidad sobre posibles factores que alteren el frente de onda del láser o su intensidad, así como saber qué características tenía dicho haz en la trampa.

También al haberse utilizado dos métodos para verter microesferas en la cavidad se pudo ver cuál era el más eficiente. Y este fue el de tener las microesferas en seco, ya que al suspenderlas en isopropanol y evaporarlo se formaban cúmulos de microesferas, los cuales eran incapaces de mantenerse en suspensión.

The purpose of this investigation was to study the oscillation of the position of the microsphere according to the fluctuations of the laser. The objective was partially fulfilled, since when analysing the data, it was observed that several data sets (according to the power of the pumping laser) presented anomalous characteristics, when the microsphere levitated they oscillated in circles. Which led to the search for a possible explanation for this anomaly and to see if there was a pattern to it. It can be concluded that the thermal lensing effect is probable, although there is no justified theory that explains the oscillations in the position of the microsphere since they are not directly due to the fluctuations of the laser. It would be necessary to carry out an in-depth study on possible factors that alter the wavefront of the laser or its intensity, as well as to know what characteristics the beam had in the trap.

Also, having used two methods to pour microspheres into the cavity, it was possible to see which was the most efficient. And this was to have them dry, since when suspending the microspheres in isopropanol and evaporating it, clusters of microspheres were formed, which were unable to stay in suspension.

Acknowledgments:

I would like to thank the Laser Spectroscopy Laboratory and High Pressures for the time of use of the equipment. I would also like to thank my tutor, Dr. Leopoldo L., for having transmitted his passion for research and for guiding me during this work.

References

[1] I. Ricardez Vargas, J.A. Carbajal Domínguez, J.A. Bernal Arroyo, J.G. Segovia López. Análisis de captura colectiva de microesferas dieléctricas en patrones ópticos 2D. Journal of Basic Sciences. 1 (1)(enero-abril 2015).

[2] Bertolotti M. The history of the laser. London, England: Institute of Physics Publishing; 2004.

[3] Ashkin A. Acceleration and trapping of particles by radiation pressure. Phys Rev Lett. 1970;24(4):156–9.

[4] Optical tweezers: where physics meets biology [Internet]. 2008 [citado 10 enero 2021]. Disponible en: https://physicsworld.com/a/optical-tweezers-where-physics-meets-biology/

[5] Ashkin A. Optical trapping and manipulation of small neutral particles using lasers. In: Frontiers in Optics 2010/Laser Science XXVI. Washington, D.C.: OSA; 2010.

[6] Chang CB, Huang W-X, Lee KH, Sung HJ. Optical levitation of a non-spherical particle in a loosely focused Gaussian beam. Opt Express. 2012;20(21):24068–84.

[7] Zhang H, Liu K-K. Optical tweezers for single cells. J R Soc Interface. 2008;5(24):671–90.

[8] Ashkin A. Forces of a single-beam gradient laser trap on a dielectric sphere in the ray optics regime. Biophys J. 1992;61(2):569–82.

[9] K. C. Neuman and S. M. Block, “Optical trapping,” 2 September 2004. Department of Biological Sciences, and Department of Applied Physics, Stanford University, Stanford, California 94305.

[10] J.F. Sánchez Ramírez, J.L. Jiménez Pérez, U. Pal, R. Gutiérrez Fuentes, J.A. Pescador Rojas and A. Cruz Orea. “Espectroscopia de lente térmica aplicada al estudio de nanofluidos conteniendo clústeres de oro”, *Revista Mexicana de Física*, 2007, 53(5), pp. 13–17.

[11] Sébastien Chénais, François Balembois, Frédéric Druon, Gaëlle Lucas-Leclin, and Patrick Georges. “Thermal Lensing in Diode-Pumped Ytterbium Lasers-Part I: Theoretical Analysis and Wavefront Measurements”, *IEEE Journal of quantum electronics,* September 2004, 40 (9), pp. 1217-1234.

[12] Jun Shen, roger D. Lowe and Richard D. Snook. “A model for cw laser induced mode-mismatched dual-beam thermal lens spectrometry”, *Chemical Physics,* 1992, 165, pp. 385-396.